

Development of high-resolution UKCIP02-based climate change scenarios in the UK

Mikhail A. Semenov*

Rothamsted Research, Harpenden, Hertfordshire AL5 2JQ, United Kingdom

Received 29 May 2006; received in revised form 20 December 2006; accepted 11 February 2007

Abstract

Analysis of possible impacts of climate change on agriculture, based on process-based simulation models, which use daily weather as their input, requires climate change scenarios with high spatial and temporal resolutions. Despite improvements in the performance of global and regional climate models, direct daily outputs from them are not suitable for such analysis. A methodology for construction of daily site-specific climate scenarios, based on a stochastic weather generator, is described. Initially the LARS-WG stochastic weather generator, used in our study, was calibrated for current climate with observed daily data. Then its parameters were adjusted for climate change, using the output from UKCIP02 projections, presented as changes in monthly mean climatic variables between the control run and future scenarios. To be able to generate scenarios at any given location in the UK, parameters of LARS-WG, computed for locations with long historical weather records, were interpolated over the UK. Distributions for climatic variables were interpolated locally and then modified by globally interpolated mean values to account for the effect of topography. As illustrations, daily UKCIP02-based scenarios were generated and used to calculate various weather extreme events and impact of climate change on wheat growth. Under a warmer climate, extreme statistics related to temperature, such as heat-waves, are likely to increase substantially in magnitude and frequency. Two impact statistics for wheat, i.e. drought stress index and probability of an episode of hot temperature after anthesis, were analysed. Despite higher temperature and lower summer precipitation for the 2080HI scenario, the relative impact on yield due to drought stress is smaller for 2080HI than for the baseline climate, because of the ability of wheat to mature early in a warmer climate avoiding summer heat and drought stress. © 2007 Elsevier B.V. All rights reserved.

Keywords: Stochastic weather generator; LARS-WG; HadRM3; Sirius; Extreme impacts; Drought stress index

1. Introduction

Many process-based models, such as crop simulation models or hydrological models, require daily site-specific weather as their input (Jamieson et al., 1998b). To use process-based models for the assessment of impacts of climate change, we have to develop climate scenarios with appropriate temporal and spatial resolutions, taking into account the model sensitivity to

variations in climatic variables. Crop simulation models incorporate a mixture of non-linear interactions between the crop and its environment (Porter and Semenov, 1999, 2005; Semenov and Porter, 1995). A non-linear model can potentially produce very different predictions depending on how climate scenarios were constructed (Mearns et al., 1997). It was demonstrated in (Porter and Semenov, 1999; Semenov and Barrow, 1997) that climate change scenarios, derived from a global climate model (GCM) that incorporated changes in climatic variability decreased mean wheat yield and significantly increased risk of crop failure compared with scenarios which accounted only for changes in

* Tel.: +44 1582763133; fax: +44 7092 287156.
E-mail address: mikhail.semenov@bbsrc.ac.uk.

mean values. Katz and Brown (1992) analysed the sensitivity of weather extreme events to changes in the mean and variability of climatic variables, and found that extreme events are more sensitive to changes in variability than to changes in the average.

The coarse spatial resolution of GCMs and large uncertainty in their output at a daily scale, particularly for precipitation, means that the daily GCM output is not appropriate directly for use with process-based models and analysis of extreme events. Despite an increasing ability of GCMs to model successfully present-day climate, the latest generation of GCMs has serious difficulties reproducing daily precipitation and temperature (Trigo and Palutikof, 2001). For example, the capacity of the Hadley Centre coupled ocean-atmosphere GCM (HadCM2) to reproduce successfully daily maximum and minimum temperature was evaluated on a seasonal basis (Trigo and Palutikof, 1999). The results for the means and variance showed significant discrepancies between the observed and HadCM2 control time series, which resulted in over-predicting the frequency of both heat-waves and cold-spells. In a different study, heat-waves and dry spells were compared for observed weather and the control Max-Planck Institute ECHAM3 GCM run (Huth et al., 2000). It was reported that in the ECHAM3 control run the heat-waves are too long, appear later in the year, peak at higher temperatures and their numbers are under- or overestimated depending on month. The simulated dry spells were also too long, and the annual cycle of their occurrence was distorted.

Regional climate models (RegCM) showed a substantial improvement in modelling spatial weather patterns compared with GCMs due to much finer spatial resolution (20–50 km). Nevertheless, an accurate reproduction of some weather statistics, including extreme events, still remains problematic. Early comparison between the RegCM (NCAR CCM) control run and observations showed that the diurnal range for temperature in the model control run is too low and the daily variability of temperature is underestimated although the daily temperature mean is often well reproduced (Mearns et al., 1995b). Different statistics of daily precipitation could lead to different conclusions about the skill of RegCM. For example, good agreement between model and observed data regarding mean daily precipitation usually results from compensating errors in the intensity and frequency fields (too high frequency and too low intensity) (Mearns et al., 1995a). More recent analysis of the Hadley Centre HadRM3H model runs showed that the HadRM3H model overestimates mean rainfall in winter and spring months, particularly at high elevations,

but underestimates rainfall in summer and autumn in the UK (Fowler et al., 2005). Precipitation biases have a detrimental effect on the simulation of drought. In particular, cumulative dry days are significantly over-estimated by the control climate simulations when compared to the observed dataset across almost the whole of the UK and particularly eastern and south-eastern regions due to the underestimation of summer and autumn rainfall by HadRM3H.

To be useful for the assessment of impact of climate change, based on process-based impact models, climate scenarios should:

- be specific to a site (1 km) with daily temporal resolution;
- include the full set of climate variables required by the impact model, e.g. minimum and maximum temperature, precipitation and radiation for crop simulation models;
- be based on GCM/RegCM predictions and incorporate changes in means and changes in climatic variability, if necessary;
- contain an adequate number of years to allow risk analysis, e.g. 100–200 years for analysis of extreme events;
- be available for any location in the region of interest.

The goal of the paper is to: (i) develop and implement a methodology for constructing high-resolution climate change scenarios for agricultural and hydrological applications, and (ii) apply climate scenarios to analyse current and future extreme weather events and to assess the impact of climate change on wheat in the UK. In Section 2 we describe a methodology for construction of climate change scenarios, which is based on a stochastic weather generator, LARS-WG (Barrow et al., 1996; Barrow and Semenov, 1995; Semenov and Barrow, 1997). The UKCIP02 projections (Hulme et al., 2002) were linked with the site-specific parameters of the LARS-WG stochastic generator, allowing generation of daily weather time series for different emission scenarios and different time periods. Spatial interpolation of parameters of LARS-WG across the UK makes it possible to generate climate scenarios for any unobserved location in the UK or any region on a grid basis (Semenov and Brooks, 1999). In Section 3 examples of the use of daily climate scenarios for analysis of weather extreme events are given. Developed scenarios were used to assess the impact of climate change on wheat in the UK using a crop simulation model, including the effects of extreme weather events.

2. Construction of daily site-specific climate change scenarios

2.1. Description of the LARS-WG stochastic weather generator

LARS-WG¹ is a stochastic weather generator based on the series approach (Racsko et al., 1991) with a detailed description being given in Semenov et al. (1998). LARS-WG produces synthetic daily time series of maximum and minimum temperature, precipitation and solar radiation. The weather generator uses available observed daily weather for a given site to determine a set of parameters for probability distributions of weather variables as well as correlations between them. After it has been obtained, this set of parameters is used to generate synthetic weather time series of arbitrary length by randomly selecting values from the appropriate distributions.

The weather generator distinguishes wet and dry days depending on whether the precipitation is greater than zero. The occurrence of precipitation is modelled by alternating wet and dry series approximated by semi-empirical probability distributions (Semenov and Brooks, 1999). On a wet day the amount of precipitation is modelled using semi-empirical distributions for each month. Minimum temperature, maximum temperature and radiation are related to the amount of cloud cover, and so LARS-WG uses separate wet and dry day distributions for each of these variables. The Normal distribution is used for the temperature variables with the mean and standard deviation varying daily according to finite Fourier series of order 3. Time auto-correlations used for minimum and maximum temperature are constant through the year and computed for each site, and the cross-correlation of the standardised residuals from the daily mean is pre-set for all sites at 0.6. Semi-empirical distributions with equal interval size are used for solar radiation (for more details see Semenov et al., 1998).

For a given set of parameters, LARS-WG produces synthetic data 1 day at a time by first determining the precipitation status of the day. The data consists of alternate wet and dry series and, when the end of one series is reached, the length of the next is chosen from the wet or dry series semi-empirical distribution for that month. For a wet day, the amount of precipitation is taken from the precipitation distribution for the month,

and the temperature and radiation values are taken from the wet day distributions and the correlation coefficients applied. The dry day distributions are applied on dry days.

The use of semi-empirical distributions gives flexibility to the generator, allowing it to model a wide variety of distributions. Analysis of observed data from many sites around the world showed that the shapes of most of the variables could vary considerably (Semenov et al., 1998). Standard distributions were only considered to be satisfactory for temperature, where the residuals are modelled by the Normal distribution and the annual variation in mean and standard deviation by Fourier series. The weather generator has been tested in diverse climates in North America, Europe, Asia and New Zealand, and was able to reproduce most of the characteristics of the observed data well at each site (Qian et al., 2004; Semenov et al., 1998).

2.2. Spatial interpolation of LARS-WG in the UK

Rather than interpolating the climate variables directly, the parameters of a weather generator for each of the observed sites can be interpolated, with the resulting new set of parameters being used by the weather generator to produce synthetic daily data for the unobserved locations (Semenov and Brooks, 1999).

The spatial interpolation procedure combines global and local interpolation. An initial local interpolation is based on sites with long daily weather records (approximately 150 weather stations were used in the UK, each with more than 20 years of daily weather). For a selected unobserved site the weighted average of each of the weather generator parameters from three neighbouring observed sites, which form a triangle containing this site, is calculated. We used the Delaunay triangulation algorithm (Delaunay, 1934), which divides the UK area into a set of adjacent triangles with vertexes at the observed sites. Similarity in the nature of the distributions of the weather variables for nearby sites is expected since the sites will normally be subject to the same basic type of weather on each day. However, systematic differences can occur particularly, if the sites are at significantly different elevations, with precipitation tending to increase and temperature and radiation tending to decrease with elevation. It is difficult to adjust the precipitation parameters using only the neighbouring sites for the difference in elevation, because the relationship varies depending on the local conditions (Daly et al., 2002, 1994).

In the global interpolation, the monthly means of precipitation, temperature and radiation data were

¹ LARS-WG is available from www.rothamsted.bbsrc.ac.uk/models/larswg.php.

spatially interpolated, using a substantially larger number of sites with monthly mean weather, and then the distributions for precipitation, temperature and radiation of the target site, derived in local interpolation, were adjusted to account for the effects of the elevation. For this purpose we used the gridded monthly climatology provided by the UK Meteorological Office (Perry and Hollis, 2004). The interpolation method used was a two-stage process of multiple regression of the climate variable (some of them were normalised first) with geographic factors as the independent variables, including an elevation along with geographical coordinates, followed by interpolation of the model residuals. The regression surface and the interpolated residual surface were added together to get the final gridded datasets. The monthly values of precipitation, minimum and maximum temperature and sunshine hours are available for 5 km grid-cells for the UK. Monthly precipitation was interpolated from 4400 sites, temperature from 430 sites and sunshine hours from 290 sites.

After local interpolation and global adjustment for the elevation, the resulting parameter file can be used by LARS-WG to generate baseline synthetic daily weather time series of any length for the target site.

2.3. UKCIP02 climate change predictions

The UKCIP02 climate change scenarios are based on a series of climate modelling experiments completed by the Hadley Centre, using HadCM3 and HadRM3 climate models (Hulme et al., 2002). These climate scenarios, based on global emissions scenarios published in 2000 by the Intergovernmental Panel on Climate Change (IPCC) in their Special Report on Emissions Scenarios (Nakicenovic and Swart, 2000), describe four alternative future climates for the UK labelled, respectively, low emissions (LO), medium-low (Med-LO) emissions, medium-high (Med-HI) emissions and high (HI) emissions and available for three time periods 2020, 2050 and 2080.

The HadCM3 global climate model is a complex tool for simulating global climate. The model is based on physical principals, describing the transport of mass and energy; these equations are solved at intervals (30 min) at a number of points forming a grid over the globe. In the HadCM3 model this grid is 2.5° in latitude \times 3.75° in longitude, corresponding to about 265 km \times 300 km over the UK. However, most processes in the atmosphere, ocean and on land, which determine climate, take place at much smaller scales. The UKCIP02 scenarios are based on the output from the regional

climate model HadRM3, which has a horizontal resolution of $0.44^\circ \times 0.44^\circ$ (50 km), and a time step of 5 min. HadRM3 takes boundary conditions from coarser resolution HadCM3 simulations and provides a higher spatial resolution of the local topography and more realistic simulations of fine-scale weather features. The advantage of this approach is that it adds physically based high-resolution information to the results of GCM experiments.

For each grid-cell UKCIP02 scenarios are provided as changes between “control” and changed HadRM3 climates for monthly mean of climatic variables, such as monthly precipitation, monthly mean minimum and maximum temperature and monthly mean radiation. These changes are provided for each time period 2020, 2050 and 2080 and for each of the emission scenarios LO, Med-LO, Med-HI and HI.

2.4. Construction of climate scenarios using LARS-WG

The changes in monthly means of climatic variables from UKCIP02 scenarios can be used to alter parameters of LARS-WG, describing present climate at a site, in a manner consistent with UKCIP02 predictions (Semenov and Barrow, 1997; Wilks, 1992). The construction of a daily climate change scenario, using LARS-WG, is a two-step procedure.

First, for a selected site ‘s’ in the UK we calculate LARS-WG parameters for baseline weather WG_s , using the interpolation procedure described above. If historical weather is available for the site, then LARS-WG can compute parameters directly using observed data. Using this set of parameters LARS-WG can generate daily site-specific weather representative to the baseline climate.

The second step is to construct a scenario file CC_s by deriving changes in mean and variability of climate variables from UKCIP02 predictions for the site ‘s’. The mean changes in total monthly precipitation, changes in monthly mean maximum and minimum temperature and changes in monthly mean radiation are available from UKCIP02 directly at 50 km grid-cells. Changes in duration of monthly mean dry and wet series, required by LARS-WG, were calculated using daily precipitation from HadRM3, which were available for the 2080 period (2065–2095). Changes in wet and dry series for 2020 and 2050 periods were obtained by the linear interpolation of the 2080s values. An example of the LARS-WG scenario file for Rothamsted for 2080HI is given in Table 1. We use the climate scenario CC_s to adjust the set of parameters WG_s at a site, producing a

Table 1

An example of the LARS-WG scenario file for Rothamsted, derived for the 2080HI projection from UKCIP02 monthly output and HadRM daily precipitation output, where Mrain is relative change in monthly mean rainfall, WetS/DryS are relative change in mean duration of wet/dry spells, T_{\max}/T_{\min} are absolute changes in daily max/min temperature and Rad is relative changes in radiation

[NAME]						
Rothamsted_HI2080						
[GCM PREDICTIONS]						
month	MRain	WetS	DryS	T_{\min}	T_{\max}	Rad
Jan	1.26	0.98	0.97	3.28	3.12	1.00
Feb	1.20	0.80	0.90	3.16	3.01	0.99
Mar	1.10	0.89	1.27	3.20	3.23	0.97
Apr	0.96	0.88	1.31	3.33	3.73	0.94
May	0.79	0.58	1.84	3.61	4.42	0.91
Jun	0.61	0.66	1.62	4.11	5.35	0.87
Jul	0.48	0.49	1.63	4.74	6.32	0.85
Aug	0.48	0.62	1.42	5.17	6.77	0.85
Sep	0.63	0.65	1.53	5.08	6.34	0.88
Oct	0.84	0.74	1.25	4.55	5.28	0.93
Nov	1.05	0.74	0.92	3.97	4.22	0.97
Dec	1.22	1.01	0.84	3.54	3.51	0.99
[END]						

new set of parameters WG_s^{CC} , which is specific to the site 's' and the scenario CC_s :

$$WG_s^{CC} = \text{adjust}(WG_s, CC_s)$$

The adjust (WG_s, CC_s) procedure is fully described in Appendix A. Using the new set of parameters WG_s^{CC} , LARS-WG can generate daily site-specific weather time series consistent with the CC_s scenario.

3. Applications and examples

To illustrate the potential use of daily site-specific climate scenarios, we compared weather extreme events and impacts on wheat for the current and future climates. We generated 150 years of daily synthetic weather for the baseline (BS), high emission scenarios for 2050 (2050HI) and 2080 (2080HI) at Rothamsted, UK, using the methodology described in Section 2. The site parameters of LARS-WG were calculated from observed daily weather at Rothamsted for 1960–1990.

3.1. Statistics of extreme weather events and impacts on wheat

We used the following statistics to compare temperature extreme events:

1. *Heat and frost indexes.* The heat index is defined as a number of days per month with maximum temperature exceeding a certain threshold T^* , e.g. $T_{\max} > T^*$.

For the frost index, we calculate a number of days per month with $T_{\min} < 0$.

2. *Heat-waves and frost-spells.* A heat-wave is defined as a continuous period (2 days or more) with daily maximum temperature exceeding 30 °C. Similar, a frost-spell is defined as a longest continuous period (2 days or more) with daily minimum temperature below 0 °C.

To compare extreme events for precipitation we use the following statistics:

1. *Daily precipitation.* We will compare 95-percentiles $R_{CC}^{0.95}$ and $R_{BS}^{0.95}$, where R stands for daily precipitation.
2. *3-Day precipitation.* For each wet series, we find the three consecutive days within the series which have the maximum total precipitation.

$$R_{3\text{days}} = \max_d \left\{ \sum_{i=1}^3 R_{d+i}, d+i \in \text{WetSeries} \right\}$$

We calculate 95-percentiles for 3-day precipitation.

We use the Sirius wheat simulation model to assess the impact of climate change on wheat. Sirius is a wheat simulation model, which predicts wheat growth and development in response to climate and environmental variations (Jamieson et al., 1998a,b; Jamieson and Semenov, 2000; Lawless et al., 2005). A brief description of Sirius and its input parameters, used in our study, are given in Appendix B. Two statistics of the climate change impact on wheat were calculated:

1. Hot temperature around anthesis can substantially reduce grain yield (Wheeler et al., 2000). Half-way through anthesis, when half of the ears in a population have flowered, temperature of 27 °C can result in a high number of sterile grains (Wheeler et al., 1996a). We calculate the probability $P_{\text{ant}+10}^{T27}$ that the maximum temperature exceeded 27 °C at least once during the 10 days after anthesis began for any single year.
2. Crop drought stress index is defined as $DSI_{\text{crop}} = Y_{\text{WL}}/Y_{\text{POT}}$, where Y_{WL} and Y_{POT} are water-limited and potential grain yields. Both yields were calculated without nitrogen limitation, and the potential yield was calculated without water limitation.

3.2. Temperature extremes

3.2.1. Heat and frost indexes

Plants could be severely damaged if daily temperature exceeds a certain temperature threshold at a certain

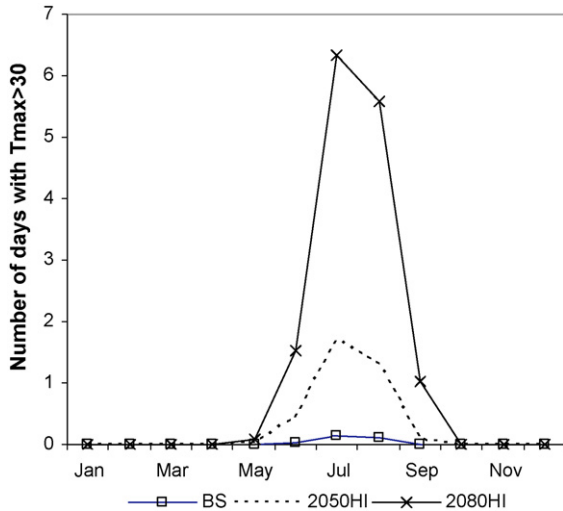


Fig. 1. Average number of days per month with maximum temperature exceeding 30° calculated for the baseline (BS), 2050HI and 2080HI scenarios at Rothamsted, UK: (\square) BS; (\cdots) 2050HI; (\times) 2080HI.

developmental stage (Porter and Gawith, 1999). It is known that many growth processes have a bell-shaped response curve to temperature with optimal growth conditions achieved when temperature is close to the middle point of the bell curve T_{opt} , and no growth when temperatures are outside the limits T_{min} and T_{max} of the curve. For example, optimal temperature for wheat growth is $17\text{--}23^{\circ}\text{C}$ over the growing season; when minimum temperature falls below 0°C or maximum temperature exceeds 37°C growth stops (Porter and Gawith, 1999). Different processes can have different temperature thresholds (Wheeler et al., 1996b). In Fig. 1 an average number of days with maximum daily temperature exceeding 30°C is shown for each month for the baseline, 2050HI and 2080HI climate scenarios. The average number of days with maximum temperature exceeding 30°C is greater than 5 in July and August for 2080HI compared with expected 0.1–0.15 days for the baseline scenario.

3.2.2. Heat-waves and frost-spells

Isolated incidents of extreme hot or cold temperatures could seriously damage a plant. A continuous period of extreme hot or cold temperature could be lethal not only for crops, but also for humans. Summer 2003 was recorded as the hottest in Europe since 1500 (Poumadere et al., 2005). The episode of heat-wave in August 2003 led to an excess of 15,000 deaths in France alone, confirming that heat-waves are a major mortality risk in post-industrial societies.

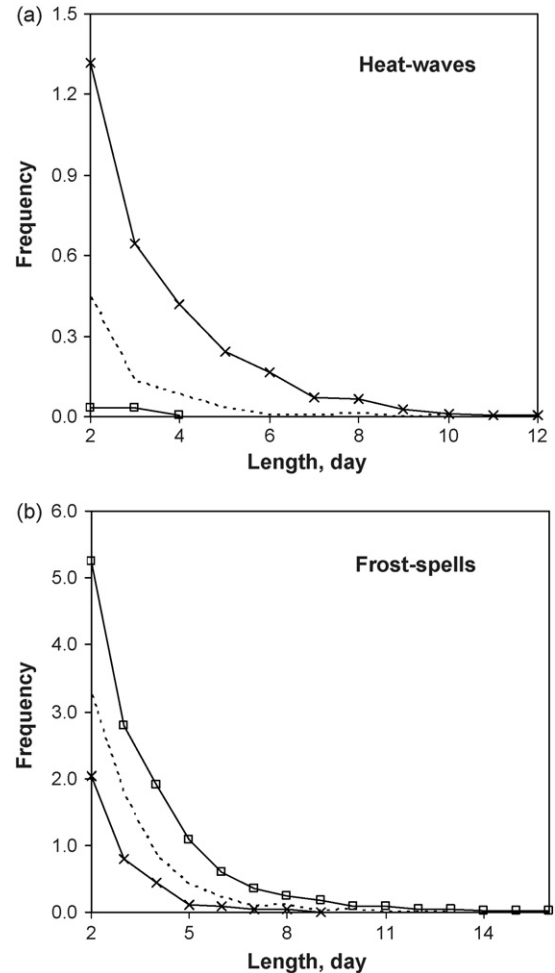


Fig. 2. Expected frequencies of (a) heat-waves with temperature exceeding 30°C and (b) frost-spells with temperature below 0°C of various lengths in a single year for the baseline (BS), 2050HI and 2080HI scenarios at Rothamsted, UK: (\square) BS; (\cdots) 2050HI; (\times) 2080HI.

Using 150 years of daily synthetic weather for the baseline, 2050HI and 2080HI scenarios at Rothamsted, we computed the expected frequency of heat-waves and cold-spells of various lengths. For the baseline climate the expected frequency of heat-waves is very low and the maximum wave was 4 days long (Fig. 2a). For the 2080HI scenario not only the frequency increased dramatically (an order of magnitude), but also the length of heat-waves (up to 12 days long) and their severity (peak temperatures during a heat-wave were higher).

Frost-spells showed an opposite tendency (Fig. 2b). The maximum length of frost-spells decreased from 18 days for baseline to 9 for 2080HI, and the frequency of frost-spells was reduced by more than half.

3.3. Precipitation extremes

Wet series are defined as series of consecutive days with precipitation greater than 0.1 mm. Changes in the mean length of dry and wet series were computed by comparing daily time series for precipitation from HadRM3 for control 1960–1990 and 2065–2095 runs (Barring et al., 2006). For the 2080HI scenario at Rothamsted the average duration of wet series is predicted to be shorter with the largest decrease of 40–50% during summer months (Table 1). The length of dry series is likely to increase by 40–60% during summer months and decrease slightly during winter months. Total monthly precipitation for the 2080HI scenario at Rothamsted is predicted to be lower by about 40–50% during summer and higher by about 20–25% during winter. The combined effect of changes in the number of wet days per month, calculated from wet and dry series, and changes in total monthly precipitation, predicted by UKCIP02, determines daily precipitation. For the 2080HI scenario mean daily precipitation is predicted to increase for all months except August. Fig. 3a shows 95-percentiles for daily precipitation for the baseline, 2050HI and 2080HI scenarios. We also calculated 95-percentiles of 3-day precipitation, as defined in Section 3.1, for each season (Fig. 3b). More intense daily precipitation (95-percentiles showed an increase for all months except August for 2080HI) or 3-day precipitation totals (for all seasons except summer—June, July and August) may have an impact on the environment and also affect agricultural crops. An increase in precipitation intensity is likely to increase N leaching with possible contamination of ground water, and the risk of soil erosion. In addition, intense rainfall can reduce availability of water for agricultural crops (given that the total monthly precipitation remains unchanged). Intense rainfall may fill up the soil water capacity with the excess water running off or percolating to deep soil layers unavailable for plants.

3.4. Impact of climate change on wheat yield

Increases in atmospheric CO₂ concentration and temperature affect potential wheat yield in opposite directions (Richter and Semenov, 2005; Semenov et al., 1993). Elevated atmospheric CO₂ concentration ([CO₂]) enhances CO₂ diffusion into the leaf and increase the photosynthetic rate of C3-plants over a wide range of radiation intensities (Ewert et al., 2002). In Sirius, radiation use efficiency (RUE) is modelled as a function of [CO₂] with the linear increase by 30%,

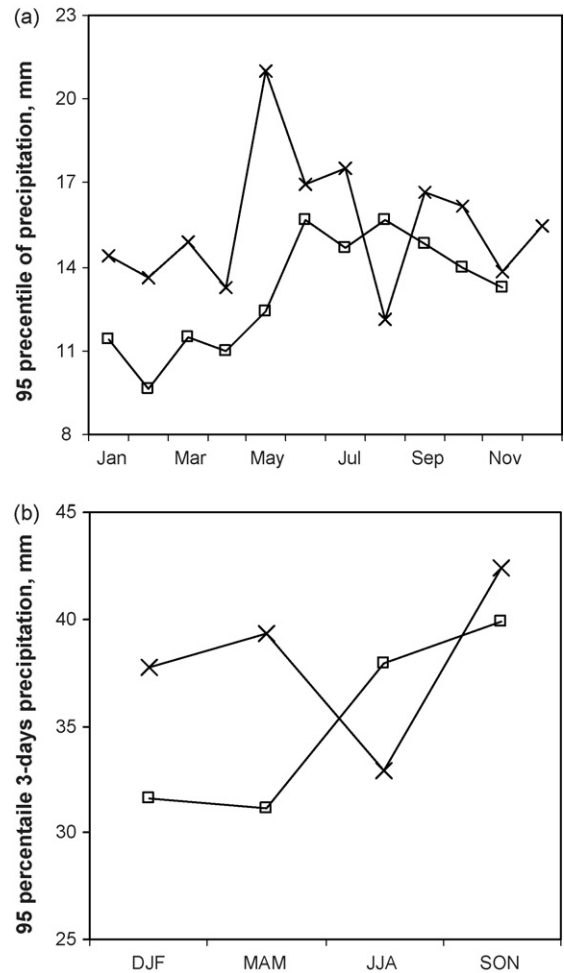


Fig. 3. (a) 95-percentile of daily precipitation calculated for each month and (b) 95-percentile of 3-day precipitation calculated quarterly (DJF = December–January–February) for the baseline (BS) and 2080HI climate scenarios at Rothamsted, UK: (□) BS; (×) 2080HI.

when [CO₂] is doubled (Lawlor and Mitchell, 1991). Wheat yield, as simulated by Sirius, increases with an increase of [CO₂].

Wheat phenology is driven by thermal time. For example, 550 °C days are typically required to complete grain filling. If temperature increases as predicted, then wheat can mature up to a month early for the 2080HI scenarios compared with the baseline climate. This has the following consequences. First, the duration of the grain filling stage, measured in calendar days, decreases resulting in the lower amount of radiation intercepted by the plant during grain filling. This, in turn, reduces production of new biomass during grain filling decreasing the final yield. Secondly, the grain filling stage will occur early in a season, when expected daily radiation is sub-optimal, i.e. lower, on average. This

Table 2

Mean of simulated wheat yield (t ha^{-1}) and its standard error (in brackets) for *cv.* Avalon and *cv.* Mercia at Rothamsted, UK calculated for 150 years of generated weather representing baseline, 2050HI and 2080HI scenarios

	Baseline (350 ppm)	2050HI (590 ppm)	2080HI (810 ppm)
Avalon			
Yield _{POT+CO₂}	9.73 (0.06)	10.38 (0.06)	11.11 (0.06)
Yield _{POT-CO₂}	9.73 (0.06)	8.61 (0.05)	7.97 (0.05)
Yield _{WL+CO₂}	9.01 (0.08)	9.81 (0.07)	10.73 (0.07)
Mercia			
Yield _{POT+CO₂}	9.75 (0.06)	10.55 (0.06)	11.00 (0.06)
Yield _{POT-CO₂}	9.75 (0.06)	8.75 (0.05)	7.89 (0.04)
Yield _{WL+CO₂}	8.79 (0.10)	9.48 (0.11)	10.07 (0.10)

Potential (POT) and water-limited (WL) yields were calculated with (+CO₂) or without (-CO₂) the effect of increase of CO₂ concentration (350, 590 and 810 ppm).

reduces grain yield even further. As a result, wheat yield decreases with global warming, if other factors are taking out of consideration.

Table 2 illustrates effects of temperature, [CO₂] and water availability on wheat yield for the baseline, 2050HI and 2080HI scenarios for *cv.* Avalon (“fast” developing variety) and *cv.* Mercia (“slow” developing variety) as simulated by Sirius (see Appendix B for more details on simulation runs). As expected mean yields for both varieties were lower for future scenarios (2050HI and 2080HI), if [CO₂] stayed on the current level of 350 ppm (Table 2, yield_{POT-CO₂}). For simulation runs, where [CO₂] was set according to the emission scenarios, both potential and water-limited yields increased for future scenarios (Table 2, yield_{POT+CO₂} and yield_{WL+CO₂}) compared with the baseline scenario. The following two examples assess the effect of high temperature and extreme drought on grain yield.

3.4.1. Hot temperature after anthesis

We used the Sirius wheat simulation model to calculate the probability of hot temperatures after anthesis $P_{\text{ant}+10}^{T27}$ defined in Section 3.1. Sirius output includes the date of anthesis, which we used to calculate

Table 3

Average date of anthesis for *cv.* Avalon and *cv.* Mercia and probability of high temperature occurring after anthesis $P_{\text{ant}+10}^{T27}$ for baseline, 2050HI and 2080HI climate scenarios (see details in the text)

	Baseline	2050HI	2080HI
Avalon			
Average date of anthesis	11 June	26 May	15 May
Probability $P_{\text{ant}+10}^{T27}$	0.121	0.154	0.242
Mercia			
Average date of anthesis	19 June	6 June	27 May
Probability $P_{\text{ant}+10}^{T27}$	0.114	0.322	0.403

for each year whether conditions for the event $P_{\text{ant}+10}^{T27}$ were satisfied. The results are presented in Table 3 for two varieties, *cv.* Avalon and *cv.* Mercia, for the baseline, 2050HI and 2080HI scenarios. For the baseline scenario $P_{\text{ant}+10}^{T27}$ equals 0.121 for *cv.* Avalon and 0.114 for *cv.* Mercia. Maximum summer temperature for 2050HI and 2080HI is substantially higher than for the baseline scenario and the 95-percentiles of maximum temperature for each summer months for 2080HI well exceed 30 °C. This affects probabilities $P_{\text{ant}+10}^{T27}$ for *cv.* Avalon and *cv.* Mercia in a different way. For the 2050HI scenario probability $P_{\text{ant}+10}^{T27}$ for *cv.* Avalon, a “fast” developing variety, only slightly increases, because *cv.* Avalon is maturing early avoiding summer heat. Probability $P_{\text{ant}+10}^{T27}$ for *cv.* Mercia, a “slow” developing variety, increased for 2050HI almost three-fold (Table 3). For the 2080HI scenario, probability $P_{\text{ant}+10}^{T27}$ for *cv.* Avalon increased two-fold compared with almost four-fold increase for *cv.* Mercia. This happened, because *cv.* Avalon reached the date of anthesis 12 days earlier than *cv.* Mercia on average for the 2080HI scenario avoiding most of the heat stress.

3.4.2. Drought stress index for wheat

Available water in the soil decreases during the growing season limiting plant growth. Different crops may respond differently to water limitation, depending on their water requirements. Therefore, the effect of drought on crops should be characterised not in terms of the soil water deficit experienced by the crop during the growing season, but by the reduction in grain yield caused by water limitation. For this reason, we calculate the wheat drought stress index $\text{DSI}_{\text{wheat}}$ (see Section 3.1). To evaluate the effect of drought on wheat growth, we ran Sirius for 150 years of the baseline and 2080HI climate scenarios at Rothamsted for water-limited and potential conditions. Cumulative distribution functions

(c.d.f.) of DSI_{wheat} are presented in Fig. 4. We used two wheat varieties, *cv.* Avalon (Fig. 4a) and *cv.* Mercia (Fig. 4b), grown on a shallow soil with low available water capacity ($AWC = 105\text{mm}$). Despite lower annual precipitation for the 2080HI climate scenario, grain yield was less affected by water stress for the 2080HI scenario for both *cv.* Avalon and *cv.* Mercia. The probability of losing 20% or more of the potential yield for *cv.* Avalon ($DSI_{\text{wheat}} = 0.8$) due to water stress is only 0.01 for the 2080HI scenario compared with 0.11 for the baseline climate (Fig. 4a). With probability 0.05 we can expect to lose 28% or more of grain yield for *cv.* Avalon due to water stress for the baseline climate, but

only 16% or more for the 2080HI scenario. Wheat matures early for the 2080HI scenario compared with the baseline, avoiding the effect of summer droughts. “Fast” developing *cv.* Avalon avoided the drought stress more successfully than “slow” developing *cv.* Mercia for future scenarios.

4. Concluding remarks

We have described the methodology for constructing daily site-specific climate change scenarios, which are suitable for impact assessment using process-based models and analysis of extreme events relevant to agriculture. The methodology is based on a stochastic weather generator. Calibrated with observed weather data a weather generator is capable to produce synthetic weather statistically similar to observed. After adjusting the weather generator baseline parameters with predicted changes in climate mean and variability, derived from global or regional climate models, a weather generator can be used to generate daily site-specific climate change scenarios. This methodology is computationally inexpensive and climate scenarios could be produced for a region or the whole UK on a high spatial resolution (e.g. 1 km grid).

For each emission scenario UKCIP02 projections were based on a single run of the Hadley Centre climate model. However, uncertainties within climate models and their parameterization exist. An approach was developed at the Hadley Centre to quantify climate model uncertainties (Harris et al., 2006). Predictions were made with large numbers of variants of the climate model, each having slightly different parameters describing the physics of the climate system. As a result, the probabilistic prediction shows the level of uncertainty in the form of a probability distribution. New scenarios describe in probabilistic terms changes in monthly means and extremes for a number of variables at 25 km resolution in the UK. The procedure, described in this paper, is flexible and could be extended to produce daily climate scenarios based on probabilistic predictions of climate change.

As an illustration daily UKCIP02-based climate scenarios for the UK were generated and used to compare various weather extreme events and extreme impacts on wheat, including intensity and occurrence of heat-waves, the drought stress index for wheat and the probability of episodes of hot temperatures after anthesis. As the climate is getting warmer, analysis showed that weather extreme statistics related to temperature, such as heat-waves, are likely to increase substantially in its magnitude and frequency. The

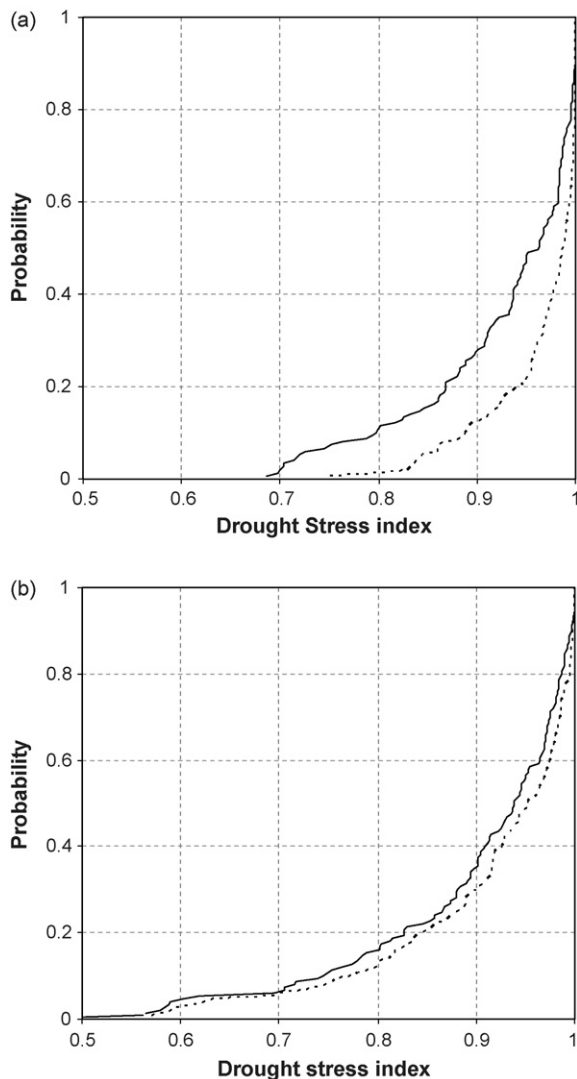


Fig. 4. Cumulative probability functions of drought stress index for wheat for the baseline (BS) and 2080HI scenarios at Rothamsted for (a) *cv.* Avalon and (b) *cv.* Mercia. Shallow soil with 105 mm available water capacity was used.

situation is more complex with climate impacts on wheat, because wheat has the ability to modify its growth and development under climate change avoiding stresses. We analysed two impact statistics for wheat, e.g. the drought stress index and the probability of an episode of hot temperature after anthesis, for two wheat varieties, *cv. Avalon* and *cv. Mercia*. Despite higher temperatures and lower summer precipitation for the 2080HI scenario, the relative reduction in grain yield due to the drought stress is shown to be smaller for 2080HI than for the baseline scenario. The explanation is that wheat matures earlier in a warmer climate, avoiding summer heat and serious drought stress. It should be noted that different wheat varieties have different abilities to mitigate climate change, e.g. *cv. Avalon*, a “fast” developing variety, is better suited to avoid summer droughts and the heat stress after anthesis than a “slow” developing *cv. Mercia*.

Acknowledgements

I thank Suzanne Clark and Sue Welham for their comments on the manuscript. Helpful comments of two anonymous reviewers are also acknowledged. Rothamsted Research receives grant-aided support from the Biotechnology and Biological Sciences Research Council of the United Kingdom.

Appendix A

We describe here how a new set of parameters $WG_s^{CC} = \text{adjust}(WG_s, CC_s)$ is calculated. Daily precipitation, length of wet and dry series and radiation are modelled, using semi-empirical probability distributions. A semi-empirical distribution $E = \{e_0, e_i; h_i, i = 1, \dots, 10\}$ is a histogram with 10 intervals $[e_{i-1}, e_i]$, where $e_{i-1} < e_i$, and h_i denotes the number of events from the observed data in the i th interval. In the case of precipitation and dry/wet series $e_0 = 0$. Minimum temperature, maximum temperature and radiation are related to the amount of cloud cover, and so LARS-WG uses separate wet and dry day distributions for each of these variables. The Normal distribution is used to model normalized residuals for temperature variables with the mean and standard deviation varying daily according to finite Fourier series of order 3.

The climate scenario file for LARS-WG $CC_s\{\text{mpr, wetS, dryS, tn, tx, rd}\}$ includes mpr – changes in monthly mean precipitation; wetS/dryS – changes in the length of wet/dry series, tn/tx – changes in monthly mean minimum and maximum temperature; rd – changes in monthly mean radiation (Table 1).

To adjust the mean of the semi-empirical distributions with the scenario value, we “stretch” the distribution changing the mean value according to the corresponding value calculated from the climate scenario file. The end points of the adjusted distribution are given by E_j and H_j , respectively, where

$$E_i = \rho e_i, \quad H_i = h_i; \quad i = 1, \dots, 10$$

where ρ is a relative predicted change in mean value. For the length of wet series ρ is calculated as

$$\rho = CC_s \cdot \text{wetS}$$

(similar for dry series). Changes in the distribution of daily precipitation are affected by changes in monthly mean precipitation $CC_s \cdot \text{mpr}$ and changes in the probability of a wet day. Therefore, for precipitation ρ is calculated as

$$\rho = CC_s \cdot \text{mpr} \frac{P_{\text{wet}}}{P_{\text{wet}}^{CC}}$$

where P_{wet} and P_{wet}^{CC} are probabilities of a wet day for the present and future climates, calculated on the basis of the LARS-WG parameters for the site and changes in the length of wet/dry series from the climate scenario CC_s :

$$\begin{aligned} P_{\text{wet}} &= \frac{\bar{S}_{\text{wet}}}{\bar{S}_{\text{wet}} + \bar{S}_{\text{dry}}}, & P_{\text{wet}}^{CC} \\ &= \frac{CC_s \cdot \text{wetS} \bar{S}_{\text{wet}}}{CC_s \cdot \text{wetS} \bar{S}_{\text{wet}} + CC_s \cdot \text{dryS} \bar{S}_{\text{dry}}} \end{aligned}$$

where \bar{S}_{wet} and \bar{S}_{dry} are mean length of wet and dry series for the baseline climate, calculated using the LARS-WG parameters. For daily radiation ρ is calculated as

$$\rho = CC_s \cdot \text{rd} \frac{\bar{R}_{\text{wet}} P_{\text{wet}} + \bar{R}_{\text{dry}} P_{\text{dry}}}{\bar{R}_{\text{wet}} P_{\text{wet}}^{CC} + \bar{R}_{\text{dry}} P_{\text{dry}}^{CC}}$$

where \bar{R}_{wet} and \bar{R}_{dry} are expected mean radiation for a wet/dry day for the baseline climate.

The shape of the daily temperature distributions for wet and dry days is approximated by the Normal distribution with the values of mean and standard deviation changing daily and calculated by a Fourier series $f(t)$ of order 3, so that

$$f(t) = \frac{1}{2} a_0 + \sum_{j=1}^3 (a_j \cos(j\omega t) + b_j \sin(j\omega t))$$

where t = Julian day, $\omega = 2\pi/365$. To adjust a maximum temperature Fourier series for future climate, we calculated new monthly mean temperature values by adding observed monthly means and corresponding

changes Δ and recalculating Fourier coefficients for new mean values. For maximum temperature Δ is calculated as

$$\Delta = CC_s \cdot tx - T_{\text{wet}}^{\text{max}}(P_{\text{wet}}^{\text{CC}} - P_{\text{wet}}) - T_{\text{dry}}^{\text{max}}(P_{\text{dry}}^{\text{CC}} - P_{\text{dry}})$$

where $T_{\text{wet/dry}}^{\text{max}}$ mean monthly maximum series for wet and dry days. Changes in minimum temperature are calculated in a similar way. The auto correlation coefficients (for minimum and maximum temperature and radiation) are kept unchanged.

Appendix B

The Sirius wheat simulation model was used in this study for quantifying the effect of climate change on wheat, including extreme impacts (Brooks et al., 2001; Jamieson et al., 1998b; Lawless et al., 2005). Sirius is a wheat model that calculates biomass from intercepted photosynthetically active radiation (PAR) and grain growth from simple partitioning rules, on a daily basis. Leaf area index (LAI) is developed from a simple canopy model (Lawless et al., 2005). Phenological development is calculated from the mainstem leaf appearance rate and final leaf number, with the latter determined by responses to daylength and vernalisation (Jamieson et al., 1998a). Effects of water and N deficits are calculated through their influences on LAI development and radiation-use efficiency (Jamieson and Semenov, 2000). Despite there being no calculation of tiller dynamics, the model accurately simulates the behaviour of crops exposed to a wide range of conditions. The model was calibrated and validated for several modern wheat cultivars and tested in many environments and climates, including Europe, New Zealand, USA and Australia and under conditions of climate change (Ewert et al., 2002; Jamieson et al., 2000; Semenov et al., 1996; Wolf et al., 1996).

Sirius requires certain data as input. It needs daily weather data (minimum and maximum temperatures, total radiation, and total rainfall). It also requires a set of cultivar parameters, which includes phyllochron, maximum canopy area, vernalisation rate parameters, daylength sensitivity and grainfill kinetic parameters. Sirius requires a description of the soil, including moisture retention properties of the soil, since they directly affect both water and nitrogen availability. And finally Sirius needs a management file, which includes sowing date, N applications and irrigations, and initial inorganic N.

For each climate scenario 150 years of synthetic daily weather were generated for Rothamsted, UK and

used as input to Sirius. We used two wheat varieties *cv.* Avalon and *cv.* Mercia, parameters of which were calibrated against agronomic experiments from the UK. The management description consisted of a sowing date of 20th October with a zero initial water deficit. We selected the Elmton soil with a low available water capacity (AWC) of 105 mm with a percolation constant of 0.4 day^{-1} and saturated moisture content and drained upper and lower limits of 56, 49 and 27%, respectively, for the top soil. Sirius was run without N limitation for all simulations. To calculate the potential yield, Sirius was run also without water limitations. Sirius accounts for different levels of CO_2 . The following levels of CO_2 were used 350, 590 and 810 ppm for the high emission scenarios for three time periods 2020, 2050 and 2080, respectively.

References

- Barring, L., Holt, T., Linderson, M.L., Radziejewski, M., Moriondo, M., Palutikof, J.P., 2006. Defining dry/wet spells for point observations, observed area averages, and regional climate model gridboxes in Europe. *Clim. Res.* 31 (1), 35–49.
- Barrow, E., Hulme, M., Semenov, M.A., 1996. Effect of using different methods in the construction of climate change scenarios: examples from Europe. *Clim. Res.* 7, 195–211.
- Barrow, E.M., Semenov, M.A., 1995. Climate change scenarios with high spatial and temporal resolution for agricultural applications. *Forestry* 68, 349–360.
- Brooks, R.J., Semenov, M.A., Jamieson, P.D., 2001. Simplifying Sirius: sensitivity analysis and development of a meta-model for wheat yield prediction. *Eur. J. Agron.* 14 (1), 43–60.
- Daly, C., Gibson, W.P., Taylor, G.H., Johnson, G.L., Pasteris, P., 2002. A knowledge-based approach to the statistical mapping of climate. *Clim. Res.* 22 (2), 99–113.
- Daly, C., Neilson, R.P., Phillips, D.L., 1994. A statistical-topographic model for mapping climatological precipitation over mountainous terrain. *J. Appl. Meteorol.* 33, 140–158.
- Delannay, B.N., 1934. Sur la sphère vide. *Izvest. Akad. Nauk SSSR* 7, 793–800.
- Ewert, F., Rodriguez, D., Jamieson, P., Semenov, M.A., Mitchell, R.A.C., Goudriaan, J., Porter, J.R., Kimball, B.A., Pinter, P.J., Manderscheid, R., Weigel, H.J., Fangmeier, A., Fereres, E., Villalobos, F., 2002. Effects of elevated CO_2 and drought on wheat: testing crop simulation models for different experimental and climatic conditions. *Agric. Ecosyst. Environ.* 93 (1/3), 249–266.
- Fowler, H.J., Ekstrom, M., Kilsby, C.G., Jones, P.D., 2005. New estimates of future changes in extreme rainfall across the UK using regional climate model integrations. 1. Assessment of control climate. *J. Hydrol.* 300 (1/4), 212–233.
- Harris, G.R., Sexton, D.M.H., Booth, B.B.B., Collins, M., Murphy, J.M., Webb, M.J., 2006. Frequency distributions of transient regional climate change from perturbed physics ensembles of general circulation model simulations. *Clim. Dynam.* 27 (4), 357–375.
- Hulme, M., Jenkins, G.J., Lu, X., Turnpenny, J.R., Mitchell, T.D., Jones, R.G., Lowe, J., Murphy, J.M., Hassell, D., Boorman, P., McDonald, R., Hill, S., 2002. Climate change scenarios for the

- United Kingdom: The UKCIP02 Scientific Report. Tyndall Centre for Climate Change Research and School of Environmental Sciences, University of East Anglia, Norwich.
- Huth, R., Kysely, J., Pokorna, L., 2000. A GCM simulation of heat waves, dry spells, and their relationships to circulation. *Climat. Change* 46 (1/2), 29–60.
- Jamieson, P.D., Berntsen, J., Ewert, F., Kimball, B.A., Olesen, J.E., Pinter, P.J.J., Porter, J.R., Semenov, M.A., 2000. Modelling CO₂ effects on wheat with varying nitrogen supplies. *Agric. Ecosyst. Environ.* 82, 27–37.
- Jamieson, P.D., Brooking, I.R., Semenov, M.A., Porter, J.R., 1998a. Making sense of wheat development: a critique of methodology. *Field Crops Res.* 55 (1/2), 117–127.
- Jamieson, P.D., Semenov, M.A., 2000. Modelling nitrogen uptake and redistribution in wheat. *Field Crops Res.* 68 (1), 21–29.
- Jamieson, P.D., Semenov, M.A., Brooking, I.R., Francis, G.S., 1998b. Sirius: a mechanistic model of wheat response to environmental variation. *Eur. J. Agron.* 8 (3/4), 161–179.
- Katz, R.W., Brown, B.G., 1992. Extreme events in a changing climate – variability is more important than averages. *Climatic Change* 21 (3), 289–302.
- Lawless, C., Semenov, M.A., Jamieson, P.D., 2005. A wheat canopy model linking leaf area and phenology. *Eur. J. Agron.* 22 (1), 19–32.
- Lawlor, D.W., Mitchell, R.A.C., 1991. The effects of increasing CO₂ on crop photosynthesis and productivity—a review of field studies. *Plant Cell Environ.* 14 (8), 807–818.
- Mearns, L.O., Giorgi, F., McDaniel, L., Shields, C., 1995a. Analysis of daily variability of precipitation in a nested regional climate model—comparison with observations and doubled CO₂ results. *Global Planet. Change* 10, 55–78.
- Mearns, L.O., Giorgi, F., McDaniel, L., Shields, C., 1995b. Analysis of variability and diurnal range of daily temperature in a nested regional climate model—comparison with observations and doubled CO₂ results. *Clim. Dynam.* 11, 193–209.
- Mearns, L.O., Rosenzweig, C., Goldberg, R., 1997. Mean and variance change in climate scenarios: methods, agricultural applications, and measures of uncertainty. *Climat. Change* 35, 367–396.
- Nakicenovic, N., Swart, R. (Eds.), 2000. *Emissions Scenarios 2000*. Special Report of the Intergovernmental Panel on Climate Change. Cambridge University Press, Cambridge, 570 pp.
- Perry, M., Hollis, D., 2004. *The Generation of Monthly Gridded Datasets for Range of Climatic Variables over the United Kingdom*. Met Office, Exeter, UK.
- Porter, J.R., Gawith, M., 1999. Temperatures and the growth and development of wheat: a review. *Eur. J. Agron.* 10 (1), 23–36.
- Porter, J.R., Semenov, M.A., 1999. Climate variability and crop yields in Europe. *Nature* 400 (6746), 724–724.
- Porter, J.R., Semenov, M.A., 2005. Crop responses to climatic variability. *Philos. Trans. R. Soc. B* 360 (1463), 2021–2035.
- Poumadere, M., Mays, C., Le Mer, S., Blong, R., 2005. The 2003 heat wave in France: dangerous climate change here and now. *Risk Anal.* 25 (6), 1483–1494.
- Qian, B.D., Gameda, S., Hayhoe, H., De Jong, R., Bootsma, A., 2004. Comparison of LARS-WG and AAFC-WG stochastic weather generators for diverse Canadian climates. *Clim. Res.* 26 (3), 175–191.
- Racsko, P., Szeidl, L., Semenov, M., 1991. A serial approach to local stochastic weather models. *Ecol. Model.* 57, 27–41.
- Richter, G.M., Semenov, M.A., 2005. Modelling impacts of climate change on wheat yields in England and Wales—assessing drought risks. *Agric. Syst.* 84 (1), 77–97.
- Semenov, M.A., Barrow, E.M., 1997. Use of a stochastic weather generator in the development of climate change scenarios. *Climat. Change* 35, 397–414.
- Semenov, M.A., Brooks, R.J., 1999. Spatial interpolation of the LARS-WG stochastic weather generator in Great Britain. *Clim. Res.* 11 (2), 137–148.
- Semenov, M.A., Brooks, R.J., Barrow, E.M., Richardson, C.W., 1998. Comparison of the WGEN and LARS-WG stochastic weather generators for diverse climates. *Clim. Res.* 10 (2), 95–107.
- Semenov, M.A., Porter, J.R., 1995. Climatic variability and the modeling of crop yields. *Agric. Forest Meteorol.* 73, 265–283.
- Semenov, M.A., Porter, J.R., Delecolle, R., 1993. Climatic change and the growth and development of wheat in the UK and France. *Eur. J. Agron.* 2, 293–304.
- Semenov, M.A., Wolf, J., Evans, L.G., Eckersten, H., Iglesias, A., 1996. Comparison of wheat simulation models under climate change. 2. Application of climate change scenarios. *Clim. Res.* 7, 271–281.
- Trigo, R.M., Palutikof, J.P., 1999. Simulation of daily temperatures for climate change scenarios over Portugal: a neural network model approach. *Clim. Res.* 13 (1), 45–59.
- Trigo, R.M., Palutikof, J.P., 2001. Precipitation scenarios over Iberia: a comparison between direct GCM output and different down-scaling techniques. *J. Clim.* 14 (23), 4422–4446.
- Wheeler, T.R., Batts, G.R., Ellis, R.H., Hadley, P., Morison, J.I.L., 1996a. Growth and yield of winter wheat (*Triticum aestivum*) crops in response to CO₂ and temperature. *J. Agric. Sci.* 127, 37–48.
- Wheeler, T.R., Craufurd, P.Q., Ellis, R.H., Porter, J.R., Prasad, P.V.V., 2000. Temperature variability and the yield of annual crops. *Agric. Ecosyst. Environ.* 82 (1/3), 159–167.
- Wheeler, T.R., Hong, T.D., Ellis, R.H., Batts, G.R., Morison, J.I.L., Hadley, P., 1996b. The duration and rate of grain growth, and harvest index, of wheat (*Triticum aestivum* L.) in response to temperature and CO₂. *J. Exp. Bot.* 47 (298), 623–630.
- Wilks, D.S., 1992. Adapting stochastic weather generation algorithms for climate changes studies. *Clim. Change* 22, 67–84.
- Wolf, J., Evans, L.G., Semenov, M.A., Eckersten, H., Iglesias, A., 1996. Comparison of wheat simulation models under climate change. 1. Model calibration and sensitivity analyses. *Clim. Res.* 7, 253–270.